# TOOL PROFILE AND TOOL PATH CALCULATION FOR FREE-FORM THICK-LAYERED FABRICATION

Imre Horváth
Joris S. M. Vergeest
Johan J. Broek
Bram de Smit

## ABSTRACT

- *In several application fields, large sized, free-form objects of various soft materials are widely used. Available layered prototyping technologies cannot be applied for fabrication of this kind of objects due to size limitations. The authors have developed a novel approach of layered manufacturing that is the most appropriate for fabrication of objects mentioned. This paper presents the algorithms for a geometrically-based modeling of the profile curve of the flexible blade tool. It also describes the algorithm for direct slicing of the CAD model and for the cusp reduction when the best fitting layer thickness is substituted by standard layer thickness. The remaining part of the paper deals with various issues of tool positioning and tool path calculation. With the developed technology $G^1$ continuity can be achieved in the internal domains of the front faces in longitudinal direction. At the transitions from one layer to the other, quasi $G^1$ continuity can be implemented. In circumferential direction $G^0$ continuity exists and further research is needed to improve it.*

## 1. INTRODUCTION

Large sized, free-form *physical models* of various soft materials (e.g., layers of plastic foam, paper, plywood, etc.) are widely used in conceptual design of automobiles and household appliances, aerodynamic and hydrodynamic simulation, decorations in the advertisement industry, scenery pieces in movie film making, and stage settings in theaters. Especially, in the entertainment industry, extra-sized human and animal mannequins and maquettes are also made of plastics. However, most of the available *layered prototyping technologies* (e.g., laser stereolitography, selective laser sintering, fused filament deposition, etc.) cannot be applied to manufacture large sized objects since they are restricted to small- or mid-size models. The general principles and these layer forming methods are described in (Kochan, D., 1993), (Chalasani, K. L., Grogan, B. N., Bagchi, A., Jara-Almonte, C. C., Ogale, A. A. and Dooley, R. L., 1991). Apparently, *thick-layered object manufacturing* (TLOM) is the best technology for the upper size domains because it gives way to decomposition and to alternative forms of materialization (e.g. solid, hollow, or reinforced shell).

Because the number of layers is proportional to the costs, efforts and time needed to manufacture, the TLOM process is in fact an optimization problem with compromises between *productivity* and *preciseness* (Wall, M. B., Ulrich, K. T. and Flowers, W. C., 1992). The closer the curvature of the cutting tool to the curved front surface of the layers, the thicker layers can be used. On the one hand, thicker layers reduce the aggregated fabrication time, on the other hand, near free-form cutting increases the cutting time of the individual layers. Nevertheless, the output and process of layered object manufacturing can be enhanced by (a) applying curved approximation for the geometric model, (b) using adaptive/segmented layer thickness calculation, (c) applying specific cutting technology to produce the curved front faces of the layers, and (d) increasing the preciseness of the assembly of the physical object.

Various types of approximation methods have already been worked out (Tangelder, J. W. H., 1998). They can be classified based on the curvedness of the approximating curve**.** The *stepped approximation* which is often referred to as *zero-order approximation* in literature is the most adequate for thin-layered deposition technologies. When the concept of *uniform slicing* is applied, it results in large errors of approximation for double-curved objects. In order to reduce the deviations, the concept of *adaptive slicing* (Suh, Y. S. and Wozny, M. J., 1994), (Kulkarni, P. and Dutta, D., 1995) has been introduced. Sabourin, E., Houser, S. A. and Bohn, J. H., (1996) presented a stepwise uniform refinement of adaptive slicing. Kulkarni, P. and Dutta, D., (1996), addressed the issue of containment to improve slicing.

To lessen the stair-case effect that is typical for stepped approximation, the concept of *ruled/sloped approximation* has been introduced. This technique is also known as *first order approximation* in literature. Object fabrication with layers of ruled front surface was extensively studied in (de Jager, P. J., 1996), (Hope, R. L., Riek, A. T. and Roth, R. N., 1996). A comparison between zero order and first order approximation techniques is presented by (de Jager P. J., Broek, J. J., Vergeest, J. S. M., 1997). Slicing calculations are typically based on .STL files that however introduce errors in approximation of the nominal shape. To avoid representation errors techniques for direct slicing of CAD models have been worked out (Vuyyuru, P., Kirschman, C. F., Fadel, G. Bagchi, A. and Jara-Almonte, C. C., 1994), (Jamieson, R. and Hacker, H., 1995). Guduri, S., Crawford, R. H. and Beaman, J. J., (1992), also addressed the issue of generating exact contour files. First order shape approximation is generally combined with adaptive slicing. *Segmentation* is typically applied to the geometric model when the shape has morphologically dissimilar domains that need significantly different layer thickness (de Jager, P. J., 1997). *Special slicing techniques*, e.g., sloped, and pie-like, can also be applied to achieve the same goal.

Recently, efforts have been made to work out techniques to improve shape approximation based on higher order curves and, at the same time, to achieve optimum layer thickness distribution. One of the techniques is based on *circular approximation* and is often called *second order approximation*. Circular approximation uses

either one circular arc, or a series of circular arcs of discrete diameters for approximation of the nominal geometry. An obvious advantage of this approach is that the type of curves used for local idealization and for approximation of the nominal geometry is actually the same. For the single arc-based approximation, the circle diameter is found from the minimum normal curvature of the shape. Curved parts of larger curvature can be cut out by using different sectors of the circular arc in a consecutive way.

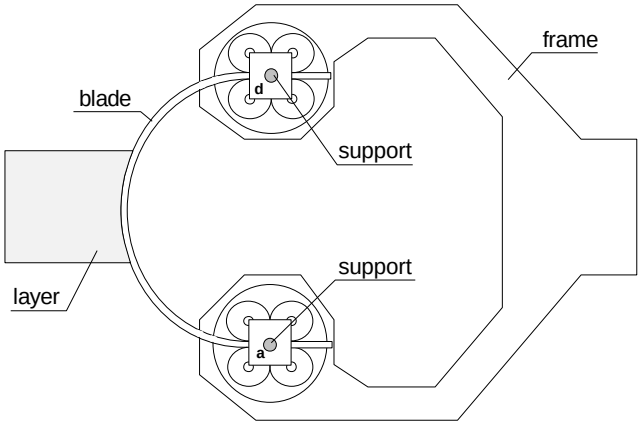


Figure 1 General arrangement of a flexible blade tool

An ultimate generalization of the shape approximation can be achieved when *higher degree curves* ($n \geq 3$) are used to approximate and carve the front surface. The curves of (n+1)-order can be of either *single polynomials* or *multi-polynomials*. In the first case higher order Bézier-curves are used, in the latter case, common or rational B-splines. The quasi-freeform manufacturing based on this higher order approximation assumes a continuous control of the shape of the tool used for cutting. Our experiments show that for free-form fabrication of plastic foam objects heated flexible blades (wires) can be applied with success. An arrangement of the flexible blade tool can be seen in Figure 1. The blade is requested to deform easily according to the shape of the front surface to be manufactured. When polynomial approximation is used, the layer thickness is calculated based on a curvature map that describes the curvature distribution profiles both in horizontal and in vertical directions of the geometric model.

## 2. PROBLEM STATEMENT

Since achieving $G^1$ (tangential) or $G^2$ (curvature) surface continuity is necessary for the large sized, free-form physical models to be manufactured from various soft materials, the authors decided to do research into the related geometric and manufacturing issues. The ultimate objective is to produce physical objects by a sort of *finish-less manufacturing*. The general problem of thick-layered object fabrication decomposes into the following sub-problems: (a) morphological analysis and evaluation of the curvature distribution of free-formed objects, (b) mathematical modeling of the shape of the flexible blade, (c) segmentation and slicing with a view to achieve balance in terms of time and preciseness of fabrication, (d) adjusting the shape of the flexible blade to local curvatures by electronic/mechanical control, (e) calculation of the tool positions, planning the tool path and technological parameters of movements/cutting, (f) manufacturing the front surfaces of the layers of various thickness, (g) assembling the layers into a physical model, and (h) finishing the

physical object. As it can be seen, the general topic of thick-layered object fabrication is much broader than that can be covered by one paper. Therefore, the authors are presenting here those results of the background research that are connected to the points (b), (c) and (e). For other details the interested reader should refer to (Horváth, I., Vergeest, J. S. M. and Juhász, I., 1998).

The main issues to elaborate on are as follows:

(a) Find a shape modeling method that is able to precisely describe the shape that corresponds to the physical behavior of the flexible blade,

(b) Work out a shape approximation method that uses the most adequate sector of the blade for approximation in order to reduce the deviance,

(c) Construct an algorithm for slicing of an object based on polynomial shape approximation and a series of layers of standard large thickness,

(d) Develop a method for calculation of the instant tool positions and the regulated tool path,

(e) Elaborate a mathematical technique for continuous setting of the profile curve of the flexible blade that can be implemented by electromechanical means.

As far as mathematical modeling of the shape of the flexible blade is concerned, the following assumptions were made:

(a) From a mechanical point of view, the blade behaves as a very slender bar which is flexible enough to take up the profile of a given shape curve, but strong enough to sustain that shape while in cutting and heated.

(b) Although its deflections are apparently large and the loads rearrange when the shape of the blade is altered, no plastic (inelastic) deformation is supposed to take place ($r \geq r_p$).

(c) The length $L$ of the blade is constant for each session of cutting with a particular tool set-up ($L = L_s$).

(d) The profile curve of the blade is jointly determined by the law of minimum strain energy under the respective circumstances ($E_s = E_{min}$) and the allowed maximum deviation $d$

(e) Albeit its instantaneous profile curve can be straight ($r = \infty$), the curved shape of the blade is not supposed to be initially straight.

(f) For symmetric setting and loading the supports result in symmetric deflection of the blade and only single inflection point is considered for stability reasons.

(g) The lateral cutting force $F$ and the bending moment $M_x$ due to $F$ cause negligible deformations on the blade. In the neighborhood of the supports, the effect of the bending moment $M_z$ can be taken into consideration by adjusting the required end slopes.

Due to the fact that the elastic deformation of the blade is comparable to its nominal size, we should have to apply the higher order deformation theory to describe the physical behavior of the shape. This complex task can be avoided by giving proper attention to the assumption (d). Furthermore, the assumption (a) implies that the cutter can be arbitrarily deformed by relatively small forces $H$ and moments $M_{bz}$ which are however larger than the cutting force $F$ and moment $M_x$ by minimum one magnitude. For its geometrically-based modeling we consider the shape of the flexible blade a planar curve and the loads acting on its very ends only. Depending on the front surface to be manufactured, the shape of the blade might have practically any shape. With a view to the tool access directions and changing the shape of the tool convexity, concavity, inflections and straightness need attention. For instance, we will not consider more complex case than curves with zero or one inflection point. The profile curve of the blade will be adjusted by (a) repositioning of the points **a** and **d** by the winding forces $H$, and (b) changing the slope (tangents $\mathbf{t}_a$ and $\mathbf{t}_d$) of the profile curve at the points **a** and **d** by bending moments $M_z$.

The calculation process of converting the CAD model to a physical model decomposes into (a) *a tool profile generation,* (b) a *shape approximation,* and (c) a *layer thickness calculation* sub-problem. The following two chapters discuss the related issues. The Chapter 6 gives the details of tool position and tool path calculation.

## 3. BOUNDARY CONFORMING APPROXIMATION OF THE FREE-FORM GEOMETRIC MODEL

### 3.1. Mathematical description of the shape approximation problem

From a mechanical point of view, the flexible blade behaves like a ‘physical spline’ which takes up its shape as governed by the law of *minimum strain energy*. It gives a possibility for us to determine the resultant curved shape by geometrically-based modeling. The shape approximation problem has been mathematically formulated as follows. Given a compound surface $F$ as an aggregation of mathematical surfaces $f_i$. Let the single connected surface **e** be one of the mathematical surfaces $f_i$ (Figure 2). Let **f** and **g** be two planar surfaces that intersect the surface **e** horizontally in curves **i** and **j**, respectively. Let a thick layer be given by $F$, **f** and **g**. Let **h** be a planar surface that is not parallel neither to **f** nor **g**. The plane **h** intersects with surface **e** in curve **q**.

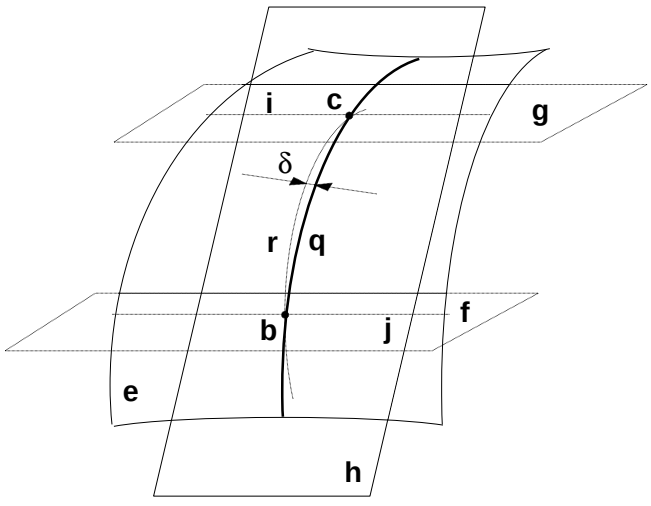


Figure 2 Arrangement for local approximation

Since **e** is supposed to be single connected, **q** is a continuous curve on **e**. Let **b** and **c** be two points on **q** as common points of surfaces **e**, **g**, **h** and **e**, **f**, **h,** respectively. Let **r** be also a planar curve in **h** that goes through the points **b** and **c** and approximates the segment of **q** falling between the points **b** and **c** with a $d$as a maximum deviation from **q**.

This shape approximation problem has two sub-problems: (a) the description of the shape of the curve **r** of constant length and minimum strain energy, and having the specified end conditions and (b) approximation of the curve **q** by curve **r** with an error less than $d$ The first sub-problem will be referred to as *curve generation*, the second as *curve matching* from now on. We assume that the locations of the two endpoints, and also the tangent directions at the ends of the blade can be directly controlled. If these two points and two directions (four 2-dimensional vectors) are specified, then the shape of the cutter, of length $L$, can be numerically approximated and represented by a planar curve **r**.

### 3.2. Calculation of the requested length of the blade

The length of the working sector of the flexible blade, $L_u$, is determined by four geometric factors, namely (a) the chosen layer thickness, (b) the global slope (calculated by averaging) or the local slope (calculated at a point **p** on the boundary curve **s**) of the front surface **e**, (c) the curvedness of the front surface **e**, and (d) the allowed deviation $\delta$ between the shape curve **q** and the profile curve **r**. At the same time, the required total length $L$ is concurrently influenced by an important technological and a mechanical aspect. The technological aspect is to enable cutting by different curved sectors of the blade by changing the tool position, but without changing the set total length $L_S$ of the blade. Using different sectors of the blade for cutting also goes together with the change in the instantaneous position of the reference point **t** of the blade. The mechanical aspect calls for shortening the length of the blade due to the risk of loosing the physical stability and stiffness when its length is large. Apparently these two aspects are working against each other, thus a compromise is to be found. Especially because the geometric factors, by forming a set of minimum requirements, do also interact with the other ones.

From geometrical point of view, the most influential is for the total length $L_S$ is the angle $a$ that varies for each shape curves **q** along the boundary curve **s**. If this angle is small, a blade of rather big length is needed which is, in turn, unfavorable from mechanical point of view. The task here is to avoid any slicing situation where the angle $\alpha$ between the bottom/top plane and the front surface of a layer is less than a given value. We applied $\alpha = 45°$as a limit value. The long blade problem however cannot be solved on the level of slicing. That is, objects of detrimental morphological characteristics must be segmented prior to slicing (Figure 3). Finding the best slicing positions for segments does help avoiding the need for extremely long blades.

The constrained blade length $L_S$ can be defined precisely if and only if the applicable standard layer thickness has already been determined. It however assumes calculation of the algebraic layer thickness that needs a predetermined (set) blade length for each layer individually. Thus, we are confronted with a recurrent procedure which can only be tackled by an initial estimation of the required blade length. The principle of estimation is shown in Figure 4.

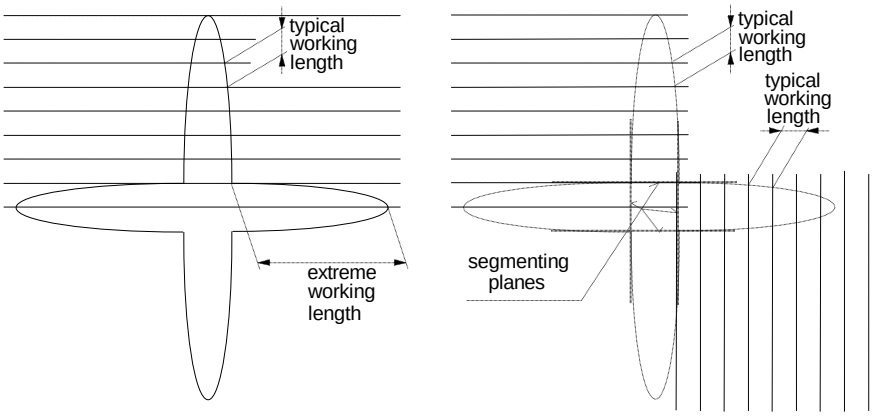


Figure 3 Avoiding unfavorable slicing situation (a) original, (b) after segmentation

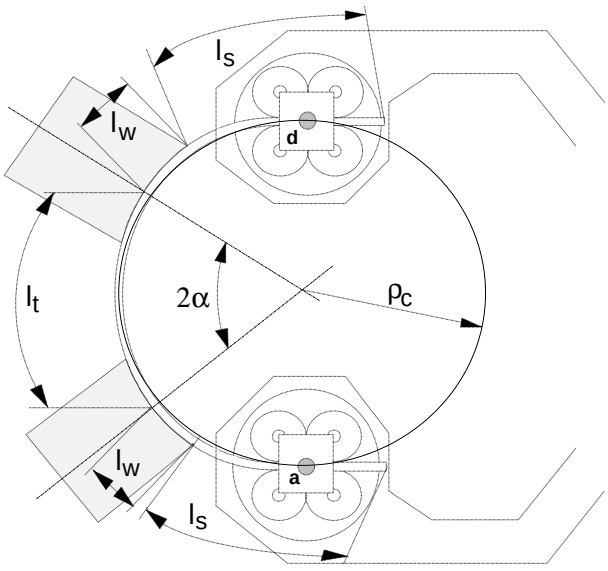


Figure 4 The principle of estimation of the required blade length

Let's assume that (a) the blade is either convex or concave, and (b) the range of swinging of the tool is 2α (in our case 90°). Let's substitute the estimated profile curve of the blade by a circle $c$ whose radius $r_c$ and center point are found by a least squares approximation of the longest shape curve on the front surface. The location of the center of the substituting circle will be at $\mathbf{r}_c = \mathbf{r} + \rho\mathbf{n}$. Let's find that cord length of the substituting circle $c$ which assures that the maximal difference between the corresponding (i.e., lying on the same horizontal line) points of the shape curve and the substituting circle is less than δ. Let the arc length $l_t$ be equal to $r_c ap/180°$. Take the one from the set $\{w_1, \ldots\ldots, w_n\}$ of the available layers of standard thickness values whose thickness $w_r$ is the nearest to the length of the cord. Denote $w_r/2$ by $l_w$. Finally, by considering the tool's geometry let's specify the length $l_s$ that is minimally requested to support the blade. Thus, the total length $L_S$ can be calculated by the following equation:

$$L_S = l_t + 2l_w + 2l_s = r_c ap/180° + w_r + 2l_s = L \quad (1)$$

In the remaining part of the paper, this estimated value $L_S$ for the individual layers is used as the tool length $L$.

### 3.3. Profile curve generation for the tool

Below, we are looking for a mathematical curve **r** that describes the physical behavior of the blade and, thus, can be considered a geometrically-based model of it. The geometrically-based modeling implies that we are not considering the actual cross section the curved blade which in addition can be circular, elliptical or diamond shape. The mechanical shape is represented by its profile curve. Without violating generality, we can assume that the curve **r** that we search for is a mapping **r(***u*) from the unit interval [0, 1] to the plane containing the blade. Let two points $\mathbf{a} \neq \mathbf{d}$ and two unit vectors $\mathbf{t}_a$ and $\mathbf{t}_d$ be given in the plane. We are looking for a curve **r**(*u*) which meets the following conditions (Figure 5):

$$\mathbf{r}(0) = \mathbf{a} \quad (2)$$

$$\mathbf{r}(1) = \mathbf{d} \quad (3)$$

$$\dot{\mathbf{r}}(0) = a\mathbf{t}_a \quad (4)$$

$$\dot{\mathbf{r}}(1) = d\mathbf{t}_d \quad (5)$$

$$\int_0^1 |\dot{\mathbf{r}}(u)| du = L \quad (6)$$

$$\int_0^1 |k(u)|^2 \, du \text{ is minimal,} \quad (7)$$

for any positive scalars *a* and *d*. Equation (7) minimizes the strain energy of **r**, which is proportional to the integrated squared curvature.

It does not seems to be feasible to find a solution to the problem in closed analytical form. It comes from the fact that Equation (7) describing the condition of minimum strain energy exclusively needs a numerical procedure even when **r** is represented in non-parametric form, i.e. **r**(*x*) = (*x*, *f*(*x*)), where *f*(*x*) is a real-valued function on the interval [$x_1$, $x_2$]. The strain energy takes the form:

$$E = c \int_{x_1}^{x_2} \frac{\left(\ddot{f}(x)\right)^2}{\left(1 + \left(\dot{f}(x)^2\right)\right)^{\frac{5}{2}}} dx . \quad (8)$$

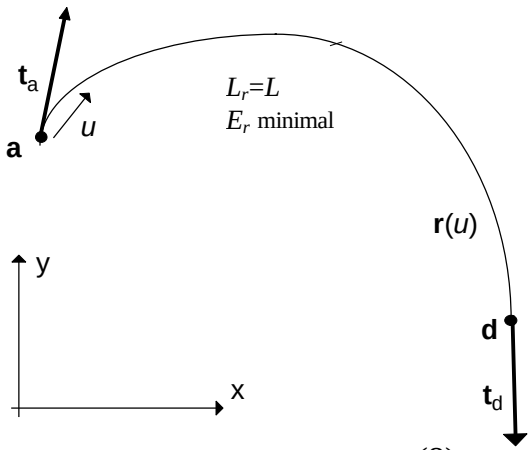


Figure 5 Curve **r** meeting the conditions (2) to (7)

The task to find the function $f(x), x \in [x_1, x_2]$ which minimizes the integral of Equation (8), is a variational problem involving

$$E(f(x)) = \int_{x_1}^{x_2} F(x; f(x), f'(x), f''(x))\,dx\,. \qquad (9)$$

The complete curve generation problem with conditions represented by Equations (2) to (7) is highly non-linear. To find a numerical solution for $\mathbf{r}(u)$, that approximately meets the conditions, we can define an objective function $F_g$ for the curve generation problem as follows;

$$F_g(v_1, \ldots, v_p) = \alpha\,|\,L_r - L\,|\; + \beta\,E_r \; + \\ + \gamma(\,|\,\mathbf{r}(0) - \mathbf{a}\,| + |\,\mathbf{r}(1) - \mathbf{b}\,|\,) \; + \; \eta(\,|\,\mathbf{t}_a - \mathbf{s}_a\,| + |\,\mathbf{t}_d - \mathbf{s}_d\,|\,), \qquad (10)$$

where the $v_i$ denote $p$ variables defining the curve $\mathbf{r}(u)$, $L_r$ is the curve length of $\mathbf{r}$ as defined in Equation (6), $E_r$ is the energy of $\mathbf{r}(u)$ as given in Equation (8) and $\mathbf{s}_a$ and $\mathbf{s}_d$ are unit tangent vectors of $\mathbf{r}$ at the points $\mathbf{r}(0)$ and $\mathbf{r}(1)$, respectively. Without loosing generality we chose these tangent vectors such that their positive directions are the same as those of the parametric derivative vectors of $\mathbf{r}(u)$ at $u = 0$ and $u = 1$. This provides an expression of $F_g$ which is independent of the parametrization $\mathbf{r}(u)$. The nonnegative scalars $\alpha$, $\beta$, $\gamma$ and $\eta$ serve to control the relative importance of the four terms when $F_g$ is minimized. The last term in Equation (10) could be slightly modified to the sum of angles rather than the sum of vector differences. Similarly, one may use squared differences in some of the penalty terms instead of the differences themselves.

If we would set $\alpha = \beta = 0$, then Equation (10) reduces to finding the Hermite interpolating $\mathbf{r}(u)$. The class of functions $\mathbf{r}(u)$ that produces $F_g = 0$ for any given endpoints and tangent vectors are the Bézier curves of degree 3. Their four control points in the plane imply $p = 8$ scalar variables for $F_g$. For this case no numerical minimization is needed; the first and last control point of $\mathbf{r}(u)$ can simply be located at $\mathbf{a}$ and $\mathbf{d}$, respectively, its second control point can be placed at $\mathbf{a} + \lambda\mathbf{t}_a$ for any positive $\lambda$, and similarly, its third control point at $\mathbf{d} - \lambda'\mathbf{t}_d$. Hence for each set of conditions expressed by Equations (2) - (5) there are infinitely many solutions $\mathbf{r}(u)$.

The next step is that we require $\mathbf{r}(u)$ to have the specified curve length $L$, i.e. condition (6), and we set $\alpha > 0$. If we then choose $\lambda = \lambda'$ for the Bézier curve just introduced, its length $L_r$ increases monotonically for increasing positive $\lambda$. Hence for any $L > |\,\mathbf{a} - \mathbf{d}\,|$ there is a unique Bézier curve of degree 3 satisfying conditions (2) to (5). To find this curve we need to iterate in the $\lambda$ space, while numerically evaluating $L_r$, see Equation (6). Here, the method of (Roulier, J. A. and Piper, B., 1996) could be applied.

Finally, by setting $\beta > 0$, we account for Equation (7), to minimize the curve's energy. Obviously, the Bézier curve $\mathbf{r}(u)$ just found may be far off the curve of minimal energy. Therefore, we need to search in a different class of curves. As discussed

in (Kallay, M., 1987) there is no reason to believe that the minimum energy curve is a piecewise polynomial. Kallay, M. therefore solved the problem by considering a general curve consisting of a finite number of linear pieces. Using a procedure in which individual pieces are translated and rotated, the polyline converged toward the minimal energy curve.

It can be expected that within the class of NURBS curves there exists a solution to the general curve generation problem, although the number of control points may get large. We investigate here two types of curves, the higher degree Bézier curves and the cubic B-spline curves. Let $\mathbf{r}(u)$ be a Bézier curve of degree $m > 2$. To make the solution to the minimization problem efficient we set the first and last control points $\mathbf{p}_0$ and $\mathbf{p}_m$ of $\mathbf{r}(u)$ to $\mathbf{a}$ and $\mathbf{d}$, respectively and we restrict $\mathbf{p}_1$ and $\mathbf{p}_{m-1}$ to be on the half lines $\mathbf{a} + \lambda\mathbf{t}_a$ and $\mathbf{d} - \lambda'\mathbf{t}_d$, respectively, where both $\lambda$ and $\lambda'$ are non-negative. The remaining $m - 3$ control points can be freely moved as to minimize $E_r$. The numerical problem thus has $p = 2 + 2(m - 3)$ scalar variables. In case of a cubic Bézier curve ($m = 3$), there are two parameters ($\lambda$ and $\lambda'$). For $m = 4$ we have two more free parameters, the co-ordinates of the middle control point of $\mathbf{r}(u)$. It can be expected that for increasing $m$, the minimal energy $E_r$ resulting from the fits will drop asymptotically toward a lower bound. However, for $m >\sim 20$, practical numerical optimizers may get unstable, not so much due to the number of parameters ($p > \sim 36$) but due to high polynomial degree of the basis functions.

To gain stability with increasing number of parameters, we may let $\mathbf{r}(u)$ be a B-spline curve of degree 3, with $n > 3$ control points $\mathbf{p}_0$ to $\mathbf{p}_{n-1.}$ We should restrict $\mathbf{p}_0$, $\mathbf{p}_1$, $\mathbf{p}_{n-2}$ and $\mathbf{p}_{n-1}$ as we did for the Bézier curve, above. The total number of variables of the problem is then $p = 2 + 2\ (n - 4)$. Now there will be no problem to use $p \approx 36$ parameters (by setting $n = 21$) since the positional and curvature evaluations do not involve high polynomial functions. B-spline curve fits involving up to 100 control points are by themselves feasible (Vergeest, J. S. M, 1989). However, besides convergence we need to consider efficiency. In principle there are additional degrees of freedom, namely the locations of the interior knots of the B-spline curve. In some situations it may be of advantage to let the knot structure deviate from being uniform. A possible drawback of the cubic B-spline curve is its inherent energy contributed by the joints between the polynomial pieces. In that case a higher degree B-spline curve could be considered.

### 3.4. Matching the profile curve to the shape curve

The curve-to-curve fitting problem can be formulated as follows. Given a curve $\mathbf{q}$ and a positive scalar $\delta$, find the curve $\mathbf{r}$ such that $D_{q,r}$ is minimal, where

$$D_{q,r} = \max_{\mathbf{p} \hat{\imath} \mathbf{q}} ( \min_{\mathbf{p}' \hat{\imath} \mathbf{r}} ( | \mathbf{p} - \mathbf{p}' | ) ) \qquad (11)$$

is a function that measures for given curves $\mathbf{q}$ and $\mathbf{r}$ their maximal positional deviation. This is a well-known problem, to which efficient solutions are available (Cox, M. G., 1986). Recent numerical applications have proven that curve-to-curve fits, using cubic B-splines for $\mathbf{r}(u)$ can be done within milliseconds for $\delta/L$ ratios of

about 0.01. In particular fast interactive sketch tools (Vergeest, J. S. M. and van Dijk, C. G. C., 1991) have been successfully implemented (van Dijk, C. G. C. and Mayer, A. A. C., 1997).

In the case of the cutter blade our initial approach to the curve matching problem is as follows. We assume that at some stage of the process to find the shape of the cutter, a candidate curve **r** has been found, which is of length $L$ and which has the minimal energy. In other words, **r** is physically feasible for certain end conditions, as described in Sub-section 3.3. We now wish to evaluate how well curve **r** approximates curve **q**, where we need to account for the fact that the length $L_q$ of **q** is different from $L$. We assume that the layer thickness is chosen such that $L_q \leq L$. Without loosing generality we may assume that, **q**($v$) is parametrized from the same domain [0, 1], as we did for **r(**$u$). The evaluation of what can be achieved with shape **r** consists of shifting curve **r** along curve **q**, in such a way that the start and endpoints **b** and **c** of **q** remain on **r** (Figure 6). A shifting algorithm can be based on the available parametrizations **r**($u$) and **q**($v$). For each shifted **r**, the value of $D_{q,r}$ needs to be calculated as follows:

$$D_{q,r'} = \max_{\mathbf{p}' \in \mathbf{q}} \left( \min_{\mathbf{p}' \in \mathbf{r}'} \left( | \mathbf{p} - \mathbf{p}' | \right) \right), \qquad (12)$$

where **r**' denotes a the particular portion of **r** that is used for the approximation of **q**. **r**'($u$) starts at **r**($u$'), for some $u$' in [0, 1). If for any such $u$' a value of $D_{q,r'}$ less than $\delta$ is obtained, a solution to the original problem is achieved. One could also choose to first check the deviation of the end tangent directions of **q**, denoted $\mathbf{t}_b$ and $\mathbf{t}_c$, respectively, from the directions of the corresponding derivative vectors of **r**($u$). Then, for the **r**($u$) with minimal tangential deviation only, the quantity $D_{q,r}$ needs to be calculated. If the smallest $D_{q,r'}$ is larger than $\delta$ then a new shape for **r** should be generated, and the process repeated. The main issue here is, how to obtain convergence in this process of combined curve generation and curve matching.

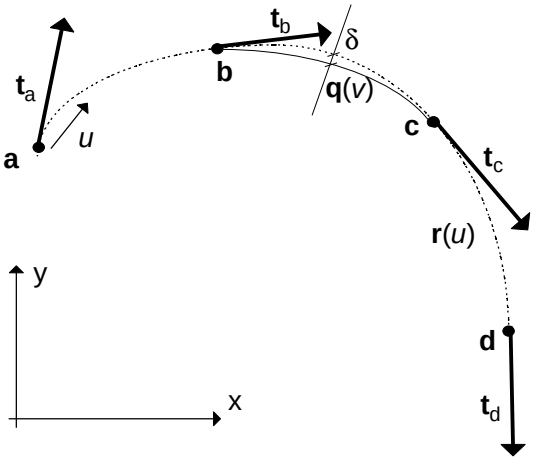


Figure 6 The given (solid) curve **q**($v$) needs to be approximated by some portion of the (dashed) curve **r**($u$).

### 3.5. Measuring the deviation between the two curves

One of the most critical parts in the numerical procedures described is the evaluation of the deviation measure $D_{q,r'}$ of Equation (12). The first issue is the specification of the begin and endpoints of portion **r**'($u$); the remaining part of **r**($u$) should be disregarded. It can be achieved by actually finding the intersection of **r**($u$) and the endpoint **c** of **q**. Then, following the principle of Equation (12), a number of points **p**' must be sampled on curve **r**'($u$), and for each **p**' its distance to curve **q** should be

calculated. This would require an iterative search by itself. An efficient approach to Equation (12) is to pre-calculate a dense set of points **p** on curve **q** and points **p'** on **r**. Since the shape of **r** during the calculation is not changed, these point set needs not to be recalculated. The min - max search of Equation (12) then comes down to a binary search in the ordered point sequences, with the opportunity to have very good start conditions from the previous search. In certain cases it may be more efficient to directly estimate the distance of points **p'** (on **r**) to curve **q**, which can be very fast if the $(x, f(x))$ property of $\mathbf{r}(u)$ can be assumed. This approach should especially be recommended if $\mathbf{r}(u)$ is not obtained as a curve proper, but as a point sequence, as is, for example, the case in the method of (Kallay, M., 1987).

### 3.6. Handling regions of specific curvature characteristics

Intuitively, singularities of a shape are discontinuities, i. e., sudden local changes that can be recognized based on the specific tangency and curvature characteristics of the domain of the shape concerned. Thus, a singularity $s$ is apparently a set of non-smooth points $\mathbf{p}_k$ of a boundary **B**, i.e., for such $\mathbf{p}_k$ there is no neighborhood $U$ in **B**, such that $\mathbf{B} \cap U$ is a manifold $C^1$ of dimension *2*. Depending on the cardinality of the set $s$ we can differentiate between zero order shape singularities $s^0$ and first order shape singularities $s^1$ (Horváth, I. and Vergeest, J. S. M., 1998). A non-smooth point $\mathbf{p} \in \mathbf{B}$ is a *zero order shape singularity* $s^0$ of ***B*** if and only if there exists a neighborhood $U \subset \Re^3$ of **p** such that $(\mathbf{B} \cap U) - \{\mathbf{p}\}$ is a $C^1$ manifold of dimension 2. This singularity type is also called *spike singularity*. A boundary **B** may have more than one spike singularity $s_{ss}$. A set $\{ \mathbf{p}_k \}$ of non-smooth points $\mathbf{p}_k \in \mathbf{B}$ is a *first order shape singularity* $s^1$ of **B** if and only if there exists a neighborhood $U \subset \Re^n$ for each $p_k$ such that $(\mathbf{B} \cap U) - \{ \mathbf{p}_k \}$ is a $C^1$ manifold of dimension 2, and $\{ \mathbf{p}_k \}$ is a $C^1$ manifold of dimension 1. This singularity type is also called *crest singularity*. A boundary **B** may have more than one crest singularity $s_{cs}$. Figure 7 presents examples of these basic types of singularities. Sub-figures 7.a1 and 7.a2 show convex and concave zero order shape singularities $s^{0c}$ and $s^{0k}$, respectively. In Sub-figures 7.b1 and 7.b2 convex and concave first order shape singularities $s^{1c}$ and $s^{1k}$ can be seen.

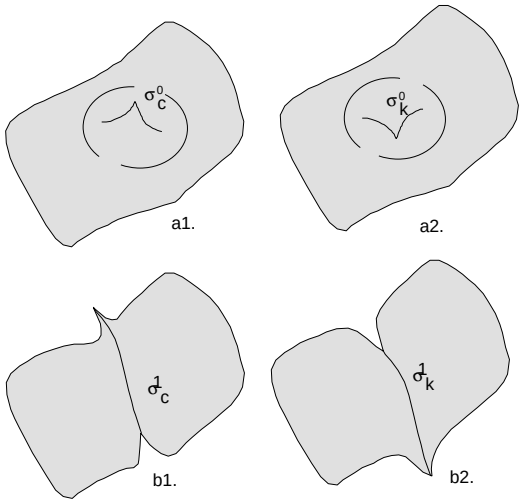

Figure 7 Types of shape singularities

When its dimensions and functionality are not really dominant compared to the whole of the object, a singularity is considered negligible. It can be ignored when shape approximation is planned and calculated. Shape discontinuities of predominant size and form need special care. Unfortunately, the approximation by continuous profile

curves raises problems in direct treatment of singularities of whichever type. A profile curve **r** of $C^1$ continuity excludes both peak singularities and crest singularities in the main plane of the blade on the front surface. The only technique for elimination of a peak singularity during slicing is to place the slicing plane upright through its tip point $p_p$. However it is of infinitely small probability that a peak singularity is located exactly at a distance that corresponds to one of the standard layer thickness from the previous slicing plane.

Treating a crest singularity is even more difficult task unless its geometric shape is a planar curve, or accidentally a straight line. In these very specific cases, letting the slicing plane through the crest singularity might be of help. Besides these cases, planar crest singularities corresponding to a given curved state of the blade can be produced by a specific (wedge-like) shaping movement of the tool. It can easily happen however that the requested wedging tool movement is hindered by shape interference. When the geometry of the crest singularity is an arbitrary spatial curve, it cannot be carved out by the thick-layered fabrication technology presented in this paper. It seems to be a possible solution to stack the semi-finished layers on each other first, and then to carve the singularity in a specific object/segment-tool arrangement and by a dedicated tool movement control. Due to these predictable difficulties, the authors believe that manufacturing of shape discontinuities cannot be fully automated.

## 4. APPROXIMATION OF THE GEOMETRIC MODEL

### 4.1. Structural decomposition

The process of thick-layered manufacturing of physical models of free-form objects starts with importing the geometric model from a commercialized CAD system. We have assumed that a NURBS representation of the model is available in a STEP file/format (Rock, S. J. and Gilman, C. R., 1995),. Later on, this exact description of the nominal geometry is used for the evaluation of structural and morphological characteristics, and also for actual slicing of the model. To facilitate shape approximation and slicing, a structurally and morphologically complex model is decomposed into less complicated components called *segments.* Segmentation depends also on the *materialization* (i.e., solid, hollow and/or reinforced) of the object which is in turn dependent both on the extent and on the morphological characteristics of the object. The necessity and/or possibility of structural decomposition is decided upon by human inspection (visual evaluation) of the CAD geometry. For separation of the segments, the geometric model is cut by sectioning planes (curved surfaces) in the CAD system and the segments are individually identified and checked for completeness. This pragmatic solution is the most useful, because any algorithm would need understanding of the topological genus of the object, interpretation of the global morphological characteristics and heuristics in problem solving.

A curvature domain oriented segmentation that is based on a formal analysis of the curvature distribution follows the structural decomposition. Both the model as a

whole and its detached components are analyzed. The algorithm is based on the evaluation of the Gaussean principal curvatures (Kulkarni, P. and Dutta, D., 1996). A *curvature map* is generated which is a multi-labelled topographic net over the boundary of the object. It specifies the location of any significant change in the normal curvatures $k_1$ and $k_2$ and also the values of radii of curvatures $r_1$ and $r_2$. Thus, the curvature map supports recognition and distinction of shape singularities of any form. Nevertheless its main purpose is to identify domains of the boundary of similar curvature characteristic. A second round of segmentation uses this information to determine segments that make shape approximation and slicing more precise. If in a front surface high-curvature regions are identified (whether or not they include singularities), then the slicing algorithm should try to break up those regions into parts that can be cut by the blade.

The choice of slicing positions influences the number of requested normal and degenerated layers and the achievable preciseness of shape approximation (Dolenc, A. and Mäkelä, I. 1994). Therefore, either for the complete model, or for its components and/or for the segments the relative optimal slicing positions are found (Frank, D. and Fadel, G. M., 1994). The position selection is relative in that sense that in the best position for slicing segments often need support *structures* (Allen, S. and Dutta, D., 1994), (Swaelens, B., Pauwels, J. and Vancraen, W., 1995).

### 4.2. Layer thickness calculation

The layer thickness calculation uses the algorithms of both curve generation and curve matching. We assume that a set W of layers of discrete (standard) thickness is available such as $W = \{w_1 , \ldots\ldots , w_n\}$, where $n \in N$. Let's also assume that decomposition of the object has happened and all of the available segments are well-shaped. The layer thickness calculation algorithm presented below is targeted to one particular segment. The Figure 8 sorts some of the possible cases of matching the the shape curve **q** to profile curve **r**. In fact, it shows the possible relationship of curves $\mathbf{q}_j$ and $\mathbf{r}_j$ at the places of significant curvature changes in the plane perpendicular to the boundary curve **s**. The possible range of layers of standard thickness are shown with dotted parallel lines. The algorithm proceeds through the steps as follows:

Assume that a plane **f** has been found that can be used as a bottom surface for the very first layer, and that it satisfies the requirements for the best slicing position. Then:

1. Take the boundary curve **s** of the segment in the plane **f**.
2. Take the curvature map and find the curvature zones $Dk_j$ in a band of width $1.5w_{max}$ along the boundary curve **s** in which the normal curvature in the longitudinal direction is *moderately variant*. A curvature zone $Dk_j$ is considered moderately variant in the longitudinal direction if the curvatures $k_j$ of two adjacent curves $\mathbf{q}_{j+1}$ and $\mathbf{q}_j$ at all of their corresponding points (sampled at distances pro-

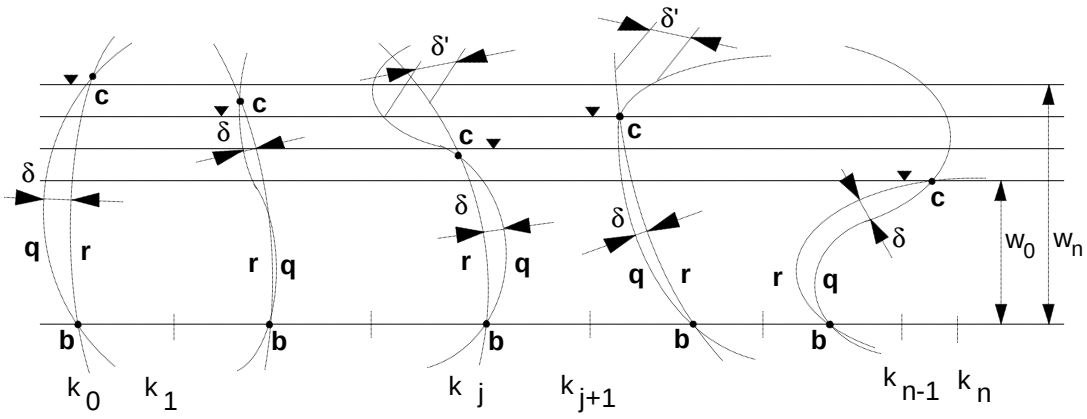


Figure 8 Standard layer thickness for different approximations

portional to their length) do not differ by more than η. That is, $\eta \geq \Delta k_{j,max} = k_{j+1,k} - k_{j,k}$ and in practice ($\eta \approx 0.1$). Indicate the limits of the zones by $k_j$.

3. For the shape curve $\mathbf{q}_j$ at $k_j$ generate an approximating profile curve $\mathbf{r}_j$.

1. Place one arbitrary point **b** of the profile curve $\mathbf{r}_j$ over the basis point **b** of the shape curve $\mathbf{q}_j$. Let's call this point as the common point **b**, from now on.
2. Rotate the profile curve $\mathbf{r}_j$ around the common point **b** until minimum one more common (intersection) point is found and the deviation δ between the corresponding points of curves $\mathbf{q}_j$ and $\mathbf{r}_j$ is less than a $\delta_0$. Call this point the point **c** afterwards.
3. If the matching described in the Step 5 failed, go to the Step 3. Otherwise, continue with the Step 7.
4. Find the distances $d_j$ between the points **c** on curves $\mathbf{q}_j$ and the plane **f** by an orthonormal projection.
5. Compare the distances $d_j$ to the maximum layer thickness $w_{max}$. If all $d_j$ are bigger than $w_{max}$, cut the segment by a plane **g**, parallel to **f**, at a distance $w_{max}$.
6. Calculate the intersection points **c'** for all curves $\mathbf{q}_j$. Check the extent of the remaining part of the segment. If it is bigger than $w_{min}$ consider the plane **g** as a new plane **f** and go to the Step 1. Otherwise continue with the Step 10.
7. Find the minimum of the distances $d_j$ and find the layer thickness for which $d_{min} \geq w$. If $d_{min} < w_{min}$ then stop. Otherwise cut the segment by a plane **g**, parallel to **f**, at a distance *w*.
8. Calculate the intersection points **c'** for all curves $\mathbf{q}_j$. Check the extent of the remaining part of the segment. If it is bigger than $w_{min}$ consider the plane **g** as a new plane **f** and go to the Step 1. Otherwise indicate insufficiency and stop.

At the end of this process, the segment is cut into layers whose front surfaces approximate the pertaining nominal surface of the CAD model with a deviation less than $d$ Due to the repositioning of the point **c** to **c'** however steps are formed because calculation for the next layer starts out of the nominal boundary curve. Mathematically, an error $m$ will most probably be found at the interface of the adjacent layers that is against the expected $G^1$ continuity.

### 4.3. Error calculation for layers with standard thickness

When a standard layer thickness is introduced as a lower bound, the actual intersection points **c'** on the curve **q** and **c"** on the curve **r** will substitute the nominal intersection point **c** (Figure 9). For instance, when $d_{min} \geq w_{max}$ the extent of the upper surface **g** will be larger than the one received when the points **c'** are exactly at a distance $w_{max}$. We call the distance between the actual points **c'** and the theoretical places of the points **c** at the same height $w$ from the bottom plane **f** (i.e., the point **c"**) a layer boundary *repositioning error m.* It has to be compensated for in order to receive minimum quasi-continuous transition, that is, an approximate $G^1$ continuity, from one layer to the other in the planes **f** and **g**. It means that the points **c'** have to be moved to the points **c"** with the calculated $m_j$ in the direction of $\overline{c'c''}$ .

In principle, there are several ways of compensating for the repositioning errors $m_j$. We have adapted the one which is the least computation-intensive. Actually the curve generation and matching procedure is not repeated, but the needed compensation is achieved by modification of the tool position in harmony with the errors $m_j$. It is also illustrated in Figure 9. The angle of the needed rotation, $\tau$, of the tool around the common point **b** can be calculated by the following equation:

$$t = arc\ tg\frac{m}{w} \tag{11}$$

where $\mu$ is the distance of $\overline{c'c''}$ . The rotation $t$ results in a displacement in the reference point **t** of the tool position which will be considered in Sub-section 5.3. as difference $\Delta\mathbf{t}^r_i$. Note that rotation of the curves $\mathbf{r}_j$ generally results in under-curved or over-curved approximation. It can be proved that the possible maximum value of $m_j$ is $m_{max} \leq d$ and it can be taken into consideration at the initial selection of the maximum value for $\delta$.

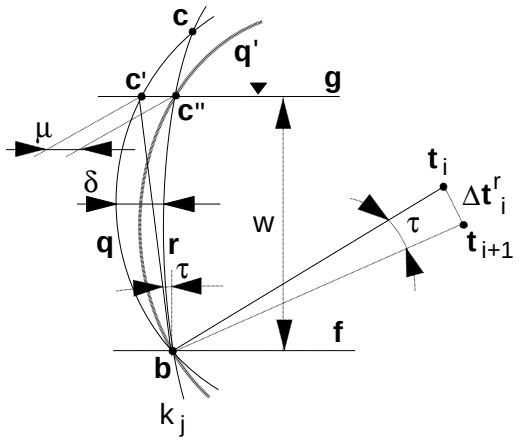


Figure 9 Calculation of the rotation of the tool for error compensation

### 4.4. Handling degenerated layers

In certain cases, domains are left in the neighborhood of the segment boundaries whose thickness $w$ is less than the available minimum layer thickness $w_{min}$. Very frequently these layers lend themselves to unfavorable cutting positions, tool orientations, and require long cutting blades. Traditional way of treating a generated layer is elimination based on rearranging the thickness of all layers involved. In our case this cannot be applied since it would demolish the achieved preciseness of approximation ( $\leq 2\delta$ ). Therefore, we apply *distinctive slicing* for degenerated layers.

The idea behind distinctive slicing is to make the use at least the minimum layer thickness $w_{min}$ and the regular tool blade profiles possible by changing the slicing direction perpendicular to the top side surface of the last layer cut. For two specific cases it is shown in Figure 10. Since degenerated layers always have a flat surface, the so called distinct layers are defined perpendicular to it. For this orthogonal layering the given range of layer thickness $W = \{w_1 , \ldots\ldots , w_n\}$ can be used together with the slicing algorithm described in the Sub-section 4.2. In this case, the evaluated layer boundary curve **s** will be a non-closed curve on the non-flat surface(s) **e**. If the stiffness or the available gripping area is not sufficient for technological reasons, it is expedient to leave the calculated *(n-1)-th* and *(n-2)-th* layers in one piece with the *n-th* degenerated layer, and apply distinctive slicing for this compound.

## 5. CALCULATION OF TOOL POSITIONS AND THE TOOL PATH

### 5.1. General arrangement

We call a given functional, geometric and positional relationship between the object to be fabricated and the flexible blade/tool at a given moment of time *situation*. For computational reasons, the continuous process of layer fabrication should be broken up a given sequence of discrete situations. The number of the requested situations is jointly influenced by the shape of the object and the preciseness to be achieved. For identifying the requested minimum number of computed situations, a threshold value in the change in the curvature is applied. Thus, a (j+1)-th situation will be identified only if the magnitude of change relative to the j-th situation exceeds a threshold value $\eta \approx 0.1$. It concerns both calculation of the tool positions and the tool path.

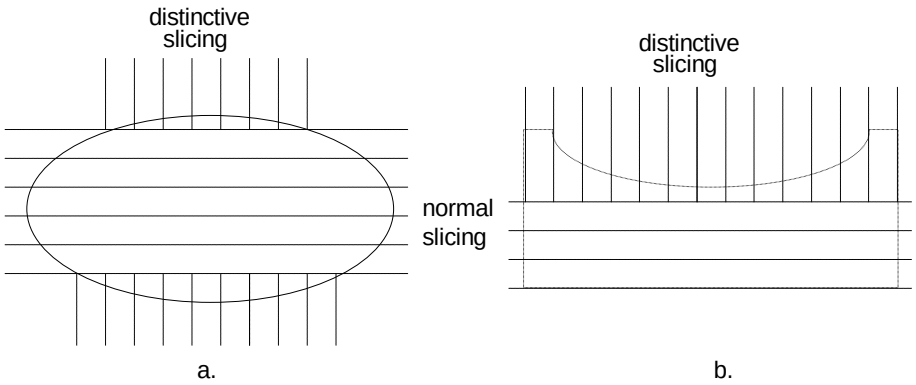


Figure 10 Distinctive slicing of the degenerated layers.

There are three reasons for a change in the tool position (translocation) between two

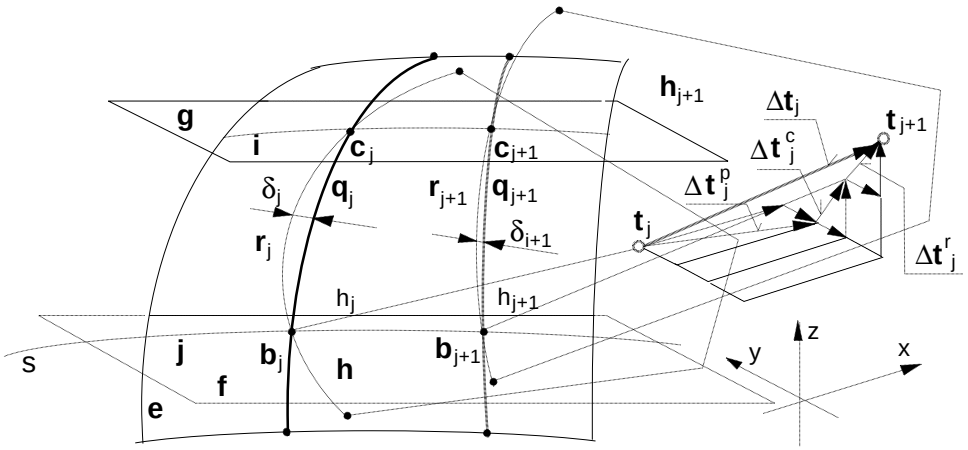


Figure 11 Change in position of the tool reference point **t** between two situations j and j+1

subsequent situations: (a) the profile curve **r** of the flexible blade has to follow the variation of the shape curve **q** to keep the allowed deviation $d$, (b) the tool has to follow the boundary curve **s** of the front surface **e** of a layer, and (c) the tool has to be rotated around the point b to compensate for the layer boundary repositioning error **s**. The difference in the positions of the reference point **t** of the tool is $\Delta\mathbf{t}^r_j$, as before. Let's denote the change due to the resetting of the blade by $\Delta\mathbf{t}^c_j$ and the change due to the tool alignment by $\Delta\mathbf{t}^p_j$. Figure 11 depicts their relation in two subsequent situations j and j+1.

For the arrangement shown in Figure 11, the resultant translocation $\Delta\mathbf{t}_j$ can be calculated as:

$$\Delta\mathbf{t}_j = \Delta\mathbf{t}^c_j + \Delta\mathbf{t}^r_j + \Delta\mathbf{t}^p_j \,. \qquad (12)$$

That is the tool position calculation task decomposes into four sub-tasks, namely, finding the values of (a) the longitudinal translocation $\Delta\mathbf{t}^c_j$, (b) the longitudinal translocation $\Delta\mathbf{t}^r_j$, (c) the circumferential translocation $\Delta\mathbf{t}^p_j$, and (d) generating the resultant translocation $\Delta\mathbf{t}_j$ of the reference point **t** of the tool. Note that for an easy verbal identification of the directions of tool movement relative to the blank layer, the notation shown in Figure 12 was introduced. While the longitudinal translocation can be calculated from the change

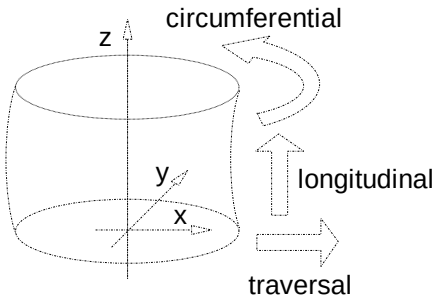


Figure 12 Notation for tool path planning

in the relative positions of the curves $\mathbf{q_i}$ and $\mathbf{r}_i$, for calculation of the circumferential translocation we need to know the boundary curve **s** of the layer, attained after slicing.

### 5.2. Calculation of the longitudinal translocation $Dt^c_i$

The absolute position of the tool reference point is defined by the vector **t**. This point **t** is the global reference point of the tool. Any translation and rotation of the tool is described by the relative positions of this point **t** as the tool is moving in the global system of co-ordinates of the fabrication equipment. Thus, let's denote $\mathbf{t}^c_i$ and $\mathbf{t}^c_{i+1}$ two subsequent positions of the tool's reference point **t** at a given $k_j$. In Figure 13, the shape curve **q** of the object to be fabricated and the blade's profile curve **r** are touching each other at the points **b** and **c**. The reference point of curve **q** is the point **v**, and its positioning point is **w**. Similarly, the reference point of curve **r** is the point **a**, and its positioning point is **d**. The points **a** and **d** are in themselves the centers of the supports of the blade on the tool body.

Knowing the reference point **a** of the curve **r** the absolute position of the reference point **t** of the tool is $\mathbf{t} = \mathbf{a} + \mathbf{h}$. However, the actual position of curve **r** is determined by its fitting to the curve **q**. Considering that the location of the reference point **v** of the curve **q** is known (since the object is supposed to be positioned in the system of co-ordinates), the vector $\mathbf{t}_i$ in a i-th situation can be expressed as:

$$\mathbf{t}^c_i = \mathbf{v} + (\mathbf{b} - \mathbf{v})_i + (\mathbf{a} - \mathbf{b})_i + \mathbf{h}. \qquad (13)$$

Then, for the (i+1)-th situation it is:

$$\mathbf{t}^c_{i+1} = \mathbf{v} + (\mathbf{b} - \mathbf{v})_{i+1} + (\mathbf{a} - \mathbf{b})_{i+1} + \mathbf{h}. \qquad (14)$$

The difference is

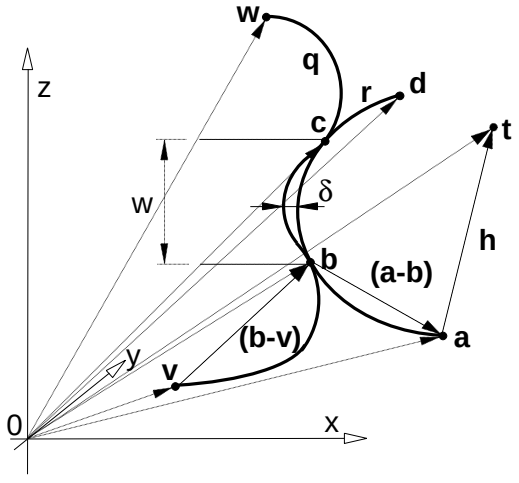


Figure 13 Finding the position of the blade's reference point **t**

$$\Delta\mathbf{t}^c_i = \mathbf{t}^c_{i+1} - \mathbf{t}^c_i$$

that is from Equations (13) and (14) is:

$$\Delta\mathbf{t}^c_i = ((\mathbf{b} - \mathbf{v})_{i+1} - (\mathbf{b} - \mathbf{v})_i) + ((\mathbf{a} - \mathbf{b})_{i+1} - (\mathbf{a} - \mathbf{b})_j)$$

Equation 16 shows that the change between two subsequent positions can be expressed by the points **a**, **b** and **v** that are points of either the curve **r** or the curve **q**, or both. Since the curves **q** and **r** are given in parametric forms, i.e., $\mathbf{q} = \mathbf{q}(v)$ and $\mathbf{r} = \mathbf{r}(u)$, the common point **b** will be on the curve **q** and the curve **r** at the parameter values $v = v_b$ and $u = u_b$.

### 5.3. Calculation of the longitudinal translocation $Dt^r_i$

Let's denote the position of the reference point **t** before rotation of the matching curve $\mathbf{r}_i$ by $\mathbf{t}^r_j$ and the position after rotation by $\mathbf{t}^r_{j+1}$ at a given $k_j$. The actual value of $\Delta t^r_i$ can be calculated by the expression:

$$\Delta \mathbf{t}^r_i = \mathbf{t}^r_{i+1} - \mathbf{t}^r_i \, . \qquad (17)$$

From the Figure 9, the angle of rotation is $\tau$, and $\mathbf{t}^r_i$ is known from Equation 13. Thus, the new position will be:

$$\mathbf{t}^r_{i+1} = \mathbf{v} + (\mathbf{b} - \mathbf{v})_i + \mathbf{R} \times ((\mathbf{a} - \mathbf{b})_i + \mathbf{h}), \qquad (18)$$

where **R** is a 2 x 2 rotation matrix of $\tau$. Finally, the longitudinal translocation $\Delta \mathbf{t}^r_i$ will be:

$$\Delta \mathbf{t}^r_i = (\mathbf{R} \times (\mathbf{a} - \mathbf{b})_i + \mathbf{h}) - ((\mathbf{a} - \mathbf{b})_i + \mathbf{h}) \qquad (19)$$

Since $\Delta \mathbf{t}^c_i$ and $\Delta \mathbf{t}^c_i$ are coplanar vectors, i.e., they are in the plane **h** of the blade, their vectorial sum is also a planar vector that can be found from Equations (16) and (19).

### 5.4. Calculation of the circumferential translocation $Dt^p_j$

The circumferential translocation of the tool depends on the arrangement and degrees of freedom of the manufacturing equipment - the selection of which is, in turn, affected by the morphological character of the layer. Based on the ratio of the width *w* and the length *l* , the form of the layer can be (a) quasi-circular - *w/l = 0.5 ¸ 2*, (b) rectangular - *w/l = 0.5 ¸ 2*, and (c) elongated - *w/l = 0.1 ¸ 20,*. For case (a) the most appropriate is a machining equipment of minimum four degrees of freedom with a rotating turn table

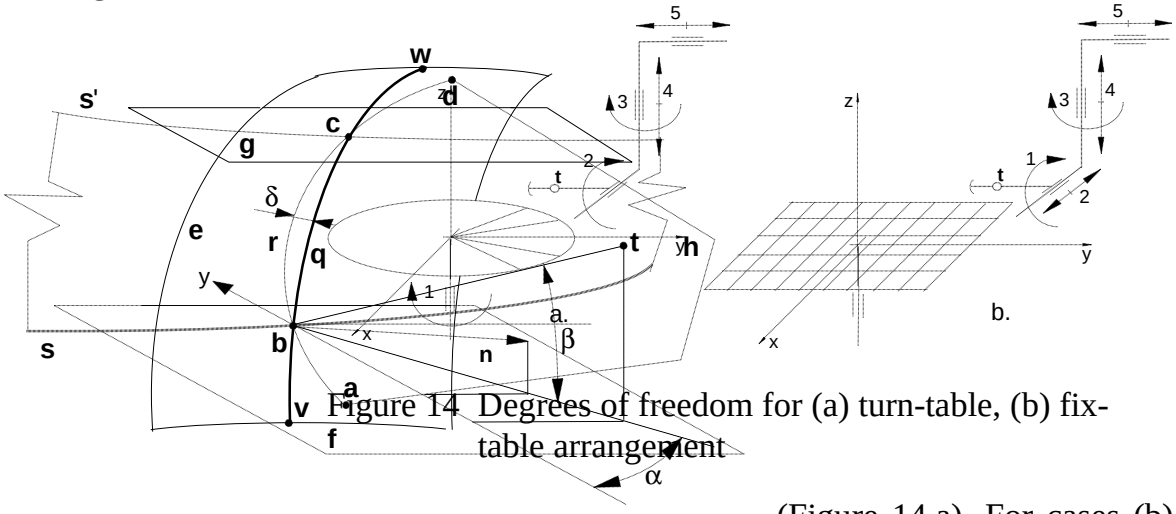


Figure 14 Degrees of freedom for (a) turn-table, (b) fix-table arrangement

Figure 15 Interpretation of the tool positioning angles *a* and *b* in $k_j$ on **s**

(Figure 14.a). For cases (b) and (c) the most adequate is

a linear (portal type) equipment of minimum four degrees of freedom with a translational turn table. The two arrangements slightly modify the way of calculation of the tool positions. For the second arrangement it can be assumed that the principal planes $\mathbf{h}_{i+1}$ and $\mathbf{h}_i$ of the tool remain parallel, but it is definitely not applicable to the first one. Therefore, the calculation is made for the more general case.

To simplify calculation, **f** is taken as parallel to the general system of coordinates. It is assumed that the plane **h** of the tool is determined by three points (**a**, **c** and **d**) of the blade and it contains the surface normal **n** of the front surface **e**. The point **b** is a point of the boundary curve **s** in the plane **f**. In order to fix the plane **h** to the general system of coordinates of the layer, we also assume that it goes through the projection of the vector **n** in the plane **f**. Thus an angle $a$ is formed between the plane **h** and the plane *yz*. Let $\beta$ be the elevation angle of the vector (**t** - **b**) from the plane xy.

The circumferential translocation $\Delta\mathbf{t}^p_j$ can be calculated from two subsequent positions of the principal plane **h** of the blade/tool along **s** (Figure 15). The actual value of $\Delta t^p_i$ can be calculated by the formula:

$$\Delta\mathbf{t}^p_j = \mathbf{t}^p_{j+1} - \mathbf{t}^p_j \,. \tag{20}$$

The place $\mathbf{t}^p_j$ of the reference point in the (j+1)-th situation is:

$$\mathbf{t}^p_{j+1} = \mathbf{b}_{j+1} + \mathbf{R}(\beta_{j+1}) \times (\mathbf{R}(\alpha_{j+1}) \times (\mathbf{t}_{j+1} - \mathbf{b}_{j+1})). \tag{21}$$

In the j-th situation $\mathbf{t}^p_j$ can be expressed by:

$$\mathbf{t}^p_j = \mathbf{b}_j + \mathbf{R}(\beta_j) \times (\mathbf{R}(\alpha_j) \times (\mathbf{t}_j - \mathbf{b}_j)). \tag{22}$$

Thus, in the plane **f** :

$$\Delta\mathbf{t}^p_j = (\mathbf{b}_{j+1} - \mathbf{b}_j) + (\mathbf{R}(\beta_{j+1}) \times (\mathbf{R}(\alpha_{j+1}) \times (\mathbf{t}_{j+1} - \mathbf{b}_{j+1})) - \\ - \mathbf{R}(\beta_j) \times (\mathbf{R}(\alpha_j) \times (\mathbf{t}_j - \mathbf{b}_j))). \tag{23}$$

By Equations (12), (16), (19) and (22) the $\Delta\mathbf{t}_j$ for all $k_j$ places can be calculated.

In practice, control of the manufacturing equipment needs global coordinate data of a given placement (position and orientation) of the layer and the tool. Therefore, it is expedient to consider a machine frame *M*, a tool frame *T*, and a layer frame *S*. The tool blade **r**, including the points **a**, **b**, **c** and **d,** is specified in the tool coordinate system *T*. The planar shape curve **q** (including the points **b** and **c**) is given in the layer coordinate system *S*. We need a software that calculates *T* and *S* relative to *M*. When the starting tool reference point **t** is known, all situation can be calculated by aggregating the differences, that is:

$$\mathbf{T}_j = \mathbf{T}_0 + \Sigma\,(\Delta\mathbf{t}_j) \tag{24}$$

The resultant tool path will result in an approximation of the nominal shape boundary as it is shown in Figure 16. If the polyline path is not sufficiently smooth, an error ς appears in the fabrication front surface. In order to regulate the tool path, adjustments should be made for the disfavor of the preciseness of shape approximation δ. The final programming of the path of the tool should extend to smoothness analysis. But detailing the method to be applied and the computer-based numerical control of the tool movement falls out of the scope of this paper.

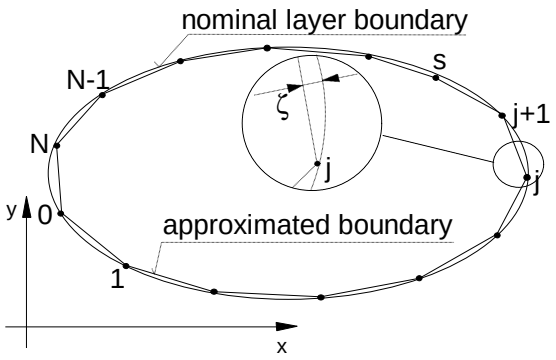


Figure 16 Result of the tool path calculation

## 6. SUMMARY AND CONCLUSIONS

Generalization of layered manufacturing and a concrete implementation for fabrication of plastic foam models have been presented. The new technology is based on (a) electronically controlled and mechanically set hot blade as an easy-to-deform cutting tool, (b) direct slicing of the CAD model (c) generation of the actual tool profile by calculating the best fitting approximation curve to the nominal shape by the principle of minimum strain energy, (d) calculation of the tool position and the tool path by the principle of maximum compensation, and (e) the use of machining equipment of high kinematic degrees of freedom. The work summarized in the paper was oriented towards a geometrically-based description of the flexible blades, slicing the CAD model into layers, and calculation of the tool positions and tool path.

We arrive at the conclusions as below:

- For large sized, free-form physical models of various soft materials fabrication based on higher order shape approximation is feasible.
- The tool (flexible blade) geometry can be generated/calculated with the assumption of minimum strain energy and specifying the boundary conditions in terms of positions of the supports, and tangency and curvature circumstances in the neighborhood of the supports.
- Curve matching uses the best fitting part of the generated profile curves in order to not to exceed the allowed deviation value, specified either for single point fit or two points fit to the nominal geometry.
- Except for some trivial cases, there is no analytical solution neither for the curve generation nor for the curve fitting problem. In order to find and solve the nu-

merical formulations of the problems, compound penalty functions are to be applied.

- If the approximation is based on multi-polynomial approach a more complex minimization problem is to be solved. Namely, if two minimal energy curves are connected with tangential continuity, then the total curve of minimal energy should be computed to the resultant of the given end conditions.
- As far as the resultant surface continuity of the object is concerned, $G^1$ continuity can be achieved in the internal domains of the front faces in longitudinal direction. In circumferential direction $G^0$ continuity exists and further research is needed to improve it. At the transitions from one layer to the other, quasi $G^1$ continuity can be implemented.
- To get the optimal result in cutting, a manufacturing equipment of high kinematical degrees of freedom is strongly recommended. The machine tool should be flexible and controllable enough to follow a continuous tool path smoothly.

Further work will focus on the smoothing of the tool path, optimization of the process parameters, further parallelization of the shape calculations and tool path calculations, and enhancement of the global throughput time.

## 7. ACKNOWLEDGMENT

The research work reported in this paper and implementation of the free-form thick-layered fabrication relates to the Integrated Concept Advancement (ICA) project of the Sub-Faculty of Industrial Design Engineering, FDEP, of the Delft University of Technology.

## 8. REFERENCES

Allen, S., Dutta, D., (1994), "On the Computation of Part Orientation Using Support Structures in Layered Manufacturing", in *Proceedings of Solid Freeform Fabrication Symposium 1994,* ed. by Marcus, H. L. et al., University of Texas, Austin, June 1994, pp. 259-269.

Chalasani, K. L., Grogan, B. N., Bagchi, A., Jara-Almonte, C. C., Ogale, A. A., Dooley, R. L., (1991), "An Algorithm to Slice 3D Shapes for Reconstruction in Prototyping Systems," *Proceedings of the 1991 ASME Computers in Engineering Conference,* August 1991, pp. 209-216.

Cox, M. G., (1986), "Data Approximation by Splines in One and Two Independent Variables", in *NPL Report DITC 7/86*, National Physics Laboratory, Teddington.

de Jager P. J., Broek, J. J., Vergeest, J. S. M., (1997), "A Comparison Between Zero and First Order Approximation Algorithms for Layered Manufacturing", *Assembly Automation*, Vol. 17, No. 3, pp. 233-238

de Jager, P. J., (1997), "Development of a New Slicing Methodology to Improve Layered Manufacturing", Ph.D. Thesis, Delft University of Technology, Delft, pp. 1-118.

Dolenc, A., Mäkelä, I. (1994), "Slicing Procedures for Layered Manufacturing Techniques", *Computer Aided Design*, Vol. 26, No. 2, pp. 119-126.

Frank, D., Fadel, G. M., (1994), "Preferred Direction of Build for Rapid Prototyping Processes", in *Proceedings of the Fifth International Conference on Rapid Prototyping*, Dayton, OH, 1994, pp. 191-200.

Guduri, S., Crawford, R. H., Beaman, J. J., (1992), "A Method to Generate Exact Contour Files for Solid Freeform Fabrication", in *Proceedings of Solid Freeform Fabrication Symposium 1992*, ed. by Marcus, H. L. et al., University of Texas, Austin, August 1992, pp. 95-101.

Hope, R. L., Riek, A. T., Roth, R. N., (1996), "Layer Building with Sloped Edges for Rapid Prototyping of Large Objects", in *Proceedings of the 5th European Conference on Rapid Prototyping and Manufacturing*, ed. by Dickens P., Helsinki, pp. 47-58.

Horváth, I., Vergeest, J. S. M., (1998), "Theoretical Fundamentals of Natural Representation of Shapes Generated with Gestural Devices", in *Proceedings of TMCE '98 Tools and Methods of Concurrent Engineering Symposium*, April 21-23, 1998, Manchester, England, pp. 17, (Status: Accepted for publication).

Horváth, I., Vergeest, J. S. M., Juhász, I., (1998), "Finding the Shape of a Flexible Blade for Free-form Layered Manufacturing of Plastic Foam Objects", in *Proceeding of the ASME 1998 Design for Manufacturing Conference*, Atlanta, Georgia, USA, September 13-16, pp. 25, (Status: Submitted for review).

Jamieson, R., Hacker, H., (1995), "Direct Slicing of CAD Models for Rapid Prototyping", *Rapid Prototyping Journal*, Vol. 1, No. 2, pp. 4-12.

Kallay, M., (1987), "Method to Approximate the Space Curve of Least Energy and Prescribed Length", *Computer-Aided Design*, Vol. 19. No. 2, pp. 73-76.

Kochan, D., (1993), "Solid Freeform Manufacturing, Advanced Rapid Prototyping", Elsevier Publishers, Amsterdam.

Kulkarni, P., Dutta, D., (1995), "Adaptive Slicing of Parametrizable Algebraic Surfaces for Layered Manufacturing", in *Proceedings of the ASME Design Engineering Technical Conferences*, Vol. 1, ed. by Azram, S. et al., ASME, New York, pp. 211-217.

Kulkarni, P., Dutta, D., (1996), "An Accurate Slicing Procedure for Layered Manufacturing", *Computer Aided Design*, Vol. 28, No. 9, pp. 683-697.

Rock, S. J., Gilman, C. R., (1995), "The Use of STEP to Integrate Design and Solid Freeform Fabrication", in Proceeding of the 1995 Solid Freeform Fabrication Sym-

posium, ed. by Marcus, H. L. et al, The University of Texas at Austin, Aug. 1995., pp. 213-220.

Roulier, J. A., Piper, B., (1996), "Prescribing the Length of Parametric Curves", *Computer Aided Geometric Design*, Vol. 13, No. 1, pp. 2-22.

Sabourin, E., Houser, S. A., Bohn, J. H., (1996), "Adaptive Slicing Using Stepwise Uniform Refinement", *Rapid Prototyping Journal*, Vol. 2, No. 4, pp. 20-26,

Suh, Y. S., Wozny, M. J., (1994), "Adaptive Slicing of Solid Freeform Fabrication Processes", in *Proceedings of the Solid Freeform Fabrication Symposium '94*, ed. by Marcus, H. L. et al., The University of Texas at Austin, Austin, pp. 404-411.

Swaelens, B., Pauwels, J., Vancraen, W., (1995), "Support Generation for Rapid Prototyping", *Proceedings of the Sixth International Conference on Rapid Prototyping*, ed. by Chartoff, R. P., Lightman, A. J., University of Dayton, June 1995, pp. 115-121.

Tangelder, J. W. H., (1998), "Decremental Physical Shape Prototyping by a Sculpturing Robot", *Ph.D. Draft Thesis*, Faculty of Design, Engineering and Production, Delft University of Technology, Delft.

van Dijk, C. G. C., Mayer, A. A. C., (1997), "Sketch Input for Conceptual Surface Design", *Computers in Industry*, Vol. 34, pp. 125-137.

Vergeest, J. S. M., (1989), "Surface Fitting for Interactive Shape Design", *Computers in Industry*, Vol. 13, No. 1, pp. 1-13.

Vergeest, J.S.M., van Dijk, C.S.G. (1991), "B-spline Surfaces for Real-time Shape Design", in *Proceedings of International Conference on Curves and Surfaces*, ed. by Laurant, P. J. et al., Chamonix-Mont-Blanc, 21-27 June 1990, Academic Press, San Diego, pp. 481-484.

Vuyyuru, P., Kirschman, C. F., Fadel, G. Bagchi, A., Jara-Almonte, C. C., (1994), "A NURBS-Based Approach For Rapid Product Realization," *Proceedings of the Fifth International Conference on Rapid Prototyping*, ed by Chartoff, R. P. et al, The University of Dayton, June 1994, pp. 229-239.

Wall, M. B., Ulrich, K. T., Flowers, W. C., (1992), "Evaluating Prototyping Technologies for Product Design", *Research in Engineering Design*, Vol. 3, No. X, pp. 163-177.

Wang, X., Cheng, F., Barsky, B. A., (1997), "Energy and B-Spline Interpolation", *Computer-Aided Design*, Vol. 29. No. 7. pp. 485-496.

## LEGEND

In the paper we are using the following notation:

- **a** the point of reference and the first support of profile curve r
- **b** one of the common points of the curves **r** and **q** and the reference point of the approximating part of the curve **r**
- **B** the boundary of an object/component/segment
- **c** one of the common points of the curves **r** and **q**
- **d** the second support of profile curve **r**
- **e** front (curved) surface of the layer
- E strain energy of the blade
- **f** bottom plane of the layer
- **g** upper plane of the layer
- **h** the position of the tool reference point **t** relative to the blade reference point **a**
- h the distance between the points **a** and **t ,** i.e., the Euclidean length ||**v**|| of the vector **v**
- L length of a curve **r**
- **p**’ points of a curve/surface
- $\mathbf{p}_i$ control points
- **q** shape curve of the object to be fabricated (mathematical)
- $\mathbf{q}_j$ discrete shape curves of the object/layer as referred to the boundary curve **s**
- **r** profile curve of the flexible blade (mathematical)
- $\mathbf{r}_i$ instantaneous profile curves of the flexible blade
- **s** boundary curve of a layer in the plane **f**
- **t** the reference point of the cutting tool
- $\mathbf{t}_x$ tangent vector at the point **x**
- **v** the reference point of the curve **q**
- **w** the positioning point of curve **q**
- w (orthonormal) layer thickness
- $\alpha$ the largest angle which can be measured between the tangent line drawn to a given point $\mathbf{p}_j$ on the front surface **e** and the intersection line of the sectioning plane *J*, containing the surface normal **n** of the surface **e,** with the base surface (bottom plane **f** or top plane **g**).
- $\delta$ orthogonal distance of a points from a curve or from a surface (in the direction of their normal vector)
- $\Delta_i$ difference in metric/parametric intervals
- $\Phi$ a front surface as an aggregation of mathematical surfaces $\phi_i$, $\Phi = \mathrm{U}\ \phi_i$
- $\eta$ curvature difference between two corresponding points of curves **q** and **r** , respectively
- $\kappa$ local curvature of a curve/surface at the points **p**’
- $\lambda_i$ scalar coefficients
- **q** plane of the blade and reference plane of the tool
- $\rho$ radius of curvature of a curve/surface ( = $1/\kappa$ )